JACS
JOURNAL OF THE AMERICAN CHEMICAL SOCIETY
Article
pubs.acs.org/JACS

Engineered Photosystem II Reaction Centers Optimize Photochemistry versus Photoprotection at Different Solar Intensities

David J. Vinyard,[†,‡,§,⊥,#] Javier Gimpel,[∥,#] Gennady M. Ananyev,[†,‡] Stephen P. Mayfield,[∥] and G. Charles Dismukes*[,†,‡]

[†]Department of Chemistry and Chemical Biology and [‡]Waksman Institute of Microbiology, Rutgers, The State University of New Jersey, Piscataway, New Jersey 08854, United States

[§]Department of Chemistry, Princeton University, Princeton, New Jersey 08540, United States

[∥]California Center for Algae Biotechnology, Division of Biological Sciences, University of California, San Diego, La Jolla, California 92093, United States

Supporting Information

ABSTRACT: The D1 protein of Photosystem II (PSII) provides most of the ligating amino acid residues for the Mn_4CaO_5 water-oxidizing complex (WOC) and half of the reaction center cofactors, and it is present as two isoforms in the cyanobacterium *Synechococcus elongatus* PCC 7942. These isoforms, D1:1 and D1:2, confer functional advantages for photosynthetic growth at low and high light intensities, respectively. D1:1, D1:2, and seven point mutations in the D1:2 background that are native to D1:1 were expressed in the green alga *Chlamydomonas reinhardtii*. We used these nine strains to show that those strains that confer a higher yield of PSII charge separation under light-limiting conditions (where charge recombination is significant) have less efficient photochemical turnover, measured in terms of both a lower WOC turnover probability and a longer WOC cycle period. Conversely, these same strains under light saturation (where charge recombination does not compete) confer a correspondingly faster O_2 evolution rate and greater protection against photoinhibition. Taken together, the data clearly establish that PSII primary charge separation is a trade-off between photochemical productivity (water oxidation and plastoquinone reduction) and charge recombination (photoprotection). These trade-offs add up to a significant growth advantage for the two natural isoforms. These insights provide fundamental design principles for engineering of PSII reaction centers with optimal photochemical efficiencies for growth at low versus high light intensities.

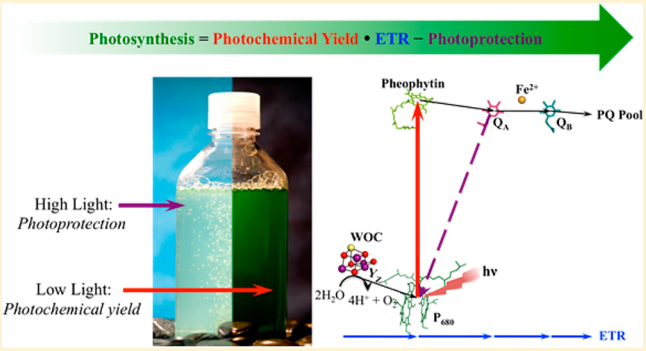

INTRODUCTION

In oxygenic photosynthesis, the pigment−protein complex Photosystem II (PSII) uses solar energy to catalyze the oxidation of water and reduction of plastoquinone (PQ). The water-oxidation complex (WOC) is a Mn_4CaO_5 cluster coupled to the primary site of photochemical charge separation (P_{680}) by a conserved redox-active tyrosine residue (D1-Y161 or Y_Z). Following four one-electron oxidations of the WOC by Y_Z and release of four protons to the lumen, one molecule of oxygen (O_2) is released.[1,2] The O_2 generated by PSII has accumulated in the oceans and atmosphere over the past ca. three billion years[3] and serves as an efficient electron sink to power heterotrophic metabolism through respiration.[4]

At the core of PSII is the D1 subunit, which provides not only most of the ligating amino acid residues to the WOC but also binding pockets for P_{680}, pheophytin (Pheo), and the secondary PQ acceptor (Q_B). The phytyl tail of the primary PQ acceptor (Q_A) is also associated with D1. The D1 polypeptide interacts with the D2 subunit and with CP43, a chlorophyll (Chl)-binding antenna subunit. Cyanobacteria are unique among oxygenic phototrophs in that they often contain multiple isoforms of the D1 protein, which are encoded by multiple *psbA* genes.[5] These *psbA* genes are differentially expressed on the basis of light intensity,[6−8] light quality,[9,10] temperature,[11] reductive stress,[12] and O_2 partial pressure.[13,14] The freshwater cyanobacterium *Synechococcus elongatus* PCC 7942 (hereafter *Synechococcus* 7942) contains two D1 isoforms: D1:1, which is expressed under normal growth conditions, and D1:2, which is expressed in response to stress (most commonly high light intensity).[6−8,15] Each isoform confers not only a fitness advantage for light utilization at its respective intensity but also a greater cellular biomass yield.[16]

The fitness advantage of each isoform is believed to be redox-controlled. *Synechococcus* 7942 D1:1 and D1:2 vary by 25 out of a total of 360 amino acids,[15] of which only residue D1-130 has

Received: January 15, 2014
Published: February 18, 2014

   dx.doi.org/10.1021/ja5002967 | *J. Am. Chem. Soc.* 2014, 136, 4048−4055

been previously studied.[17−20] Residue D1-130 is hydrogen-bonded to Pheo,[17] and in D1:1 it is a Gln, while in D1:2 it is a Glu.[5] This amino acid substitution has been hypothesized to account for the −17 mV shift in the Pheo/Pheo$^-$ midpoint reduction potential (E_m) between D1:1 and D1:2 in isolated reaction centers from *Thermosynechococcus elongatus* BP-1.[21,22] However, when only the D1:2-E130Q point mutation was made in *T. elongatus*, E_m(Pheo/Pheo$^-$) was changed by −30 mV.[20] This result is in good agreement with a previous study in which a Q130E point mutation in *Synechocystis* sp. PCC 6803 changed E_m(Pheo/Pheo$^-$) by +33 mV.[17] The less dramatic change in E_m(Pheo/Pheo$^-$) between D1:1 and D1:2 compared with D1:2-E130Q and D1:2 strongly suggests that other amino acid differences between the D1 isoforms affect the Pheo environment and thus its E_m. Revealing the influence of such amino acid substitutions was a key motivator of the present work.

Recently, we introduced a robust *Chlamydomonas reinhardtii* (hereafter *Chlamydomonas*) chloroplast expression system for expressing *psbA* variants in a uniform green algal background.[16,23] In the present study, we used this system to analyze a suite of point mutations in order to explore which of the 25 amino acid substitutions between D1:1 and D1:2 impact the previously observed phenotypes. We found that in addition to residue D1-130, D1-152 is critically important for the photochemical quantum yield at high or low light intensity. An analysis of D1:1, D1:2, and seven point mutants made in the D1:2 background allowed us to make statistically significant correlations between the PSII photochemical quantum yield, WOC cycle period, WOC turnover probability, O_2 evolution rate, and tolerance to photoinhibition. These correlations reveal the trade-offs in performance between photochemical yield and tolerance to photoinhibition, thus providing the fundamental design principles for engineering of PSII reaction centers with optimal photosynthetic efficiencies for growth at either low or high light intensities.

METHODS

Mutant Construction. A *Chlamydomonas* strain generated from wild-type 137c (CC-125 mt+) in which both *psbA* copies had been inactivated and a single copy of the native gene had been reintroduced at a neutral site in the chloroplast genome was available from a previous study.[24] Herein we refer to this strain as "*C.r.*". *Chlamydomonas* strains expressing heterologous *psbA* sequences from *Synechococcus* 7942 were previously described[16] and in this work are termed D1:1 and D1:2. All point mutations were generated in the D1:2 *psbA* sequence as described in Figure S2 in the Supporting Information using standard overlap-extension polymerase chain reaction (PCR).[25] The D1 C-terminal peptide extension from *Chlamydomonas* was constant in all of the constructs (Figure S2). The mutated genes (including their endogenous regulatory regions) were cloned into a *Chlamydomonas* transformation vector by the USER cloning technique.[26] Transformations were carried out using biolistics, and initial selection was performed on kanamycin plates. Single colonies were then transferred to minimal medium for assessment of autotrophy.[23] All of the transformations resulted in rescue of photosynthesis and were confirmed by sequencing of the PCR-amplified *psbA* insertion after at least three growth passages.

Culturing Conditions. Strains were grown photoautotrophically under 80 μE m^{-2} s^{-1} of continuous photosynthetically active radiation in HS medium[27] supplemented with 5 mM $NaHCO_3$ at 25 ± 1°. Cultures were bubbled with 2% CO_2 in humidified sterile air at a flow rate of approximately 200 mL/min. For growth experiments, full growth curves were recorded by monitoring the optical density at 730 nm (OD_{730}) and then fit to a four-component Gompertz function.[28] The dry weight at stationary phase was determined gravimetrically from filtered cells dried overnight at 90°. For all other analyses, semicontinuous cultures were maintained by daily dilution of each culture so that experiments were performed on early exponential cells, defined as OD_{730} = 0.150 ± 0.025. The Chl content was determined spectrophotometrically by methanol extraction using extinction coefficients from Porra.[29]

Western Blots. Quantitative anti-D1 Western blots were performed on thylakoid membrane preparations as previously described[30] with the following modifications. Early exponential cells were concentrated by centrifugation and then resuspended in protein extraction buffer (62.5 mM Tris, pH 6.8, 300 mM sucrose, 10 mM dithiothreitol). Cells were lysed by three rounds of snap freezing in liquid N_2 and sonication just until thawed. Samples were centrifuged at 20000*g* for 10 min, and the supernatant was discarded. The resulting thylakoid membranes were solubilized in protein extraction buffer plus 2% lithium dodecyl sulfate (LiDS), and the solution was subjected to one round of snap freezing and sonication. Samples were centrifuged at 20000*g* for 10 min to remove cell debris. Into each well of a 4−20% Tris-glycine NUView precast gel was loaded 0.1 μg total Chl, and the gel run at 200 V for 45 min at 4°. Proteins were electrophoretically transferred to a PVDF membrane, which was then blocked in 5% nonfat dry milk. The primary antibody was an anti-D1 rabbit polyclonal antibody targeting the conserved D1 C-terminus (Agrisera, Vännäs, Sweden), and detection was facilitated by a horseradish peroxidase-conjugated anti-rabbit goat IgG secondary antibody (GeneTex, Irving, CA). Amersham ECL Prime and Amersham ECL Hyperfilm (GE Healthcare, Piscataway, NJ) were used for luminescence detection. Each experiment included a five-point calibration curve of D1 standard protein (His-tagged *Synechocystis* sp. PCC 6803 D1, Agrisera), which enabled sample quantification by densitometry using ImageJ (http://rsb.info.nih.gov/ij/).

O_2 Evolution Rates. Steady-state O_2 evolution rates were measured from early exponential whole cells in HS medium supplemented with 5 mM $NaHCO_3$ at 25° using a commercial Clark electrode (Hansatech). Continuous saturating illumination was provided by a red light-emitting diode (LED) (680 μE m^{-2} s^{-1}, λ_{max} = 627 nm). Determinations of O_2 evolution rates [measured as μmol of O_2 (mg of Chl)$^{-1}$ h^{-1}] and Western blot analyses (providing Chl/PSII ratios) were performed on identical cultures and used to calculate the O_2 evolution rates (in units of O_2 PSII^{-1} s^{-1}).

Fast Repetition Rate (FRR) Fluorometry. FRR fluorometry measurements were performed on early exponential whole cells in standard medium (HS supplemented with 5 mM $NaHCO_3$) as previously described.[31] This protocol is summarized in Figure S1 in the Supporting Information and includes a one-second exposure of blue light before each two-minute dark adaptation period. This method not only prevents physiological adaptation to the generally dark measurement conditions but also ensures that Y_D is oxidized at the beginning of each single-turnover flash (STF) train. The Chl-a variable fluorescence yield, F_v/F_m, was measured on each STF using 60 μs pulses at 656 nm. F_v/F_m was calculated from the first-flash (dark-adapted) value (F_o) and the light-saturated value (F_m) from each flash in the train of flashes, with $F_v = F_m - F_o$ (see Figure S1). The WOC turnover period was determined by Fourier transform,[31] and the WOC turnover probability was quantified by analytical fitting of the flash-induced oscillations in the amplitude of F_v/F_m to the VZAD extended Kok model using the S-state eigenvalues of asymmetric Markov matrices (STEAMM) algorithm.[32] The light-limited WOC turnover efficiency was measured at a low flash rate (0.2 Hz) where it is lowered because of charge recombination reactions involving metastable oxidation states (the S_2 and S_3 states).[31]

Photoinhibition. Sensitivity to photoinhibition was determined by temporal tracking of F_v/F_m losses during exposure to saturating light from a red LED panel (300 μE m^{-2} s^{-1}, λ_{max} = 620 nm) in the presence of the chloroplast protein synthesis inhibitor lincomycin.[33−35] Each 3 mL aliquot of early exponential whole cells was treated with 1 mM lincomycin and then exposed to photoinhibitory light for 18 min. The sample was then moved to a commercial PAM fluorometer (Photon Systems Instruments, Brno, Czech Republic) and

dx.doi.org/10.1021/ja5002967 | J. Am. Chem. Soc. 2014, 136, 4048−4055

dark-adapted for 2 min, after which F_v/F_m was measured. This process (18 min light, 2 min dark) was repeated over a 2 h period. The decreasing values of F_v/F_m over time were fit to a one-component exponential decay function.

RESULTS

Selection of Point Mutations. Amino acid residue 130 was mutated in the D1:2 *psbA* gene from Glu to Gln (D1:2-E130Q), analogous to that present in native D1:1 (Figure S2 in the Supporting Information). However, the resulting phenotype, which is detailed in the following sections, was more severe than that observed for D1:1 (lower photochemical quantum yield, lower O_2 evolution rate, more sensitive to photoinhibition, and reduced growth rate). These results are in agreement with the hypothesis[20] that the other 24 amino acid variants between D1:1 and D1:2 provide compensating residues that counteract the deleterious effects of Gln at position 130.

Because individually mutating all 25 amino acid variants in all combinations between D1:1 and D1:2 is impractical, we focused on residues that shared common structural features and were highly conserved. A survey of 58 cyanobacterial D1 sequences containing Glu130 and 42 containing Gln130 showed that D1:2 residues were more conserved in these 25 positions than in D1:1, and hence, we chose the former isoform as the target for our mutational analysis. As shown in Figure S2 in the Supporting Information, seven of the 25 amino acid variants between the two isoforms are localized to the interface between the CP43 core antenna and D1 at positions 121, 123, 124, 151, 152, 155, and 288. These seven residues in the D1:2 sequence were collectively mutated to the corresponding D1:1 residues, generating the D1:2-3-helix strain. A second strain was created that also incorporated the D1:2-E130Q point mutation (D1:2-3-helix+E130Q).

After observing that the 3-helix mutations rescued the E130Q phenotype (detailed in the following sections), we analyzed these seven amino acid residues for evolutionary conservation among cyanobacteria containing both D1:1 and D1:2. Differential expression of *psbA* genes encoding D1:1 and D1:2 in response to light intensity has been experimentally observed in *Synechococcus* 7942,[7] *T. elongatus* BP-1,[36] and *Anabaena* sp. PCC 7120.[37] Of the available genomes in CyanoBase,[38] it was determined that six other cyanobacteria likely contain this simple D1:1/D1:2 expression system. The criteria used for this analysis were as follows: (a) one or more identical *psbA* gene(s) with Gln at position 130; (b) one or more identical *psbA* gene(s) with Glu at position 130; and (c) no other *psbA* genes. Ambiguous assignments (e.g., two unique *psbA* genes, both with Gln130) were excluded. The genomes that met these criteria include *S. elongatus* PCC 6301, *Synechococcus* sp. CC9902, *Synechococcus* sp. CC9311, *Synechococcus* sp. RCC307, *Synechococcus* sp. WH8102, and *Synechococcus* sp. WH7803. As graphically represented in Figure S4 in the Supporting Information, a significant fraction of D1:1 and D1:2 sequences both contain Ile at positions 121 and 123. Additionally, at position 124, eight of the nine D1:1 sequences contain Ser, while all nine D1:2 sequences contain a bulky residue (five with Phe and four with Tyr). Substitution of Val in D1:2 for Leu in D1:1 at position 151 is completely conserved in this sample set. At position 152, seven of the nine D1:1 sequences contain Ser, while all nine D1:2 sequences contain Ala. Substitutions at position 155 are generally less conserved, with D1:1 sequences having Phe (five of nine), Met (three of nine), or Thr (one of nine) and D1:2 sequences having either Ser (five of nine) or Thr (four of nine). At position 288, all nine D1:2 sequences contain Leu, while seven of the nine D1:1 sequences contain Met.

This analysis indicates that the substitutions at positions 124, 151, 152, and 288 are most highly conserved. In view of the large changes in side-chain chemistry between residues at 124 (Ser vs Phe for D1:1 and D1:2, respectively) and 152 (Ser vs Ala for D1:1 and D1:2, respectively), we chose to first make these individual point mutations. D1:2-F124S and D1:2-A152S were therefore generated both individually and in combination with D1:2-E130Q (Figure S2 in the Supporting Information).

PSII Quantum Yield and Light-Limited WOC Turnover Efficiency. The Chl-a variable fluorescence yield, F_v/F_m, is proportional to the PSII photochemical (charge separation) quantum yield.[39] In FRR fluorometry with flashes shorter than the water oxidation cycle steps, F_v/F_m exhibits period-four oscillations due to differential fluorescence quenching by the water cycle intermediates (S_i states).[31] The damping of F_v/F_m oscillations in the *C.r.*, D1:1, and D1:2 strains was previously shown to significantly vary only at low flash frequencies ($\leq$0.5 Hz), reflecting competing charge recombination under light-limiting conditions.[16] We therefore performed FRR fluorometry experiments for the strains described in this work at 0.2 Hz, where appreciable recombination contributes, and fitted the results to the model to determine the average hit parameter ($\gamma_{0.2\ Hz}$) (see Methods). Less damping reflects higher WOC turnover efficiency and is quantified by a higher probability to advance to the next oxidation state (γ). The rate of damping of F_v/F_m is the same as the rate of damping of the flash O_2 yield, indicating that both methods reflect the WOC turnover efficiency.[2,16,31] As shown in Figure 1a, D1:2 has an initial F_v/F_m value of 0.403 on the first flash (dark-preadapted) and exhibits period-four oscillations that are damped with an average hit parameter ($\gamma_{0.2\ Hz}$) of 0.492 (Figure 1b) and a period (P) of 4.81 (Figure 1c). When residue 130 is mutated to Gln (D1:2-E130Q), the initial F_v/F_m decreases to 0.279, but the quality of the period-four oscillations improves to $\gamma = 0.630$ and $P = 4.55$ (Figure 1a,b). On the other hand, when position 152 is mutated to Ser (D1:2-A152S), the initial F_v/F_m increases to 0.492, but the quality of oscillations decreases to $\gamma = 0.268$ and $P = 5.21$ (Figure 1a,b). When both mutations are made (D1:2-A152S+E130Q), the initial F_v/F_m and γ are statistically identical to those of the original D1:2 strain (Figure 1a,b).

Full FRR fluorescence traces and fits to a thermodynamically accurate Kok cycle[32] at 0.2 Hz for all nine strains are provided in Figure S5 in the Supporting Information, and the results are summarized in Figure 2b. The WOC turnover periods were determined by Fourier transforms of these data for all strains and are shown in Figure 2a. The phenotype of D1:2-F124S (in terms of both F_v/F_m and γ) was not substantially different from that of D1:2, nor was D1:2-F124S+E130Q substantially different from D1:2-E130Q. The 3-helix phenotype (alone or in combination with E130Q) was similar to the A152S phenotype. Figure 2a shows a clear positive correlation between the WOC turnover period at 0.2 Hz and the photochemical quantum yield for D1:1, D1:2, and the point mutants [$R^2 = 0.9232$, $\alpha < 0.0001$, where α is the probability of a type-I (false-positive) error[40]]. As shown in Figure 2b, the WOC turnover probability at 0.2 Hz ($\gamma_{0.2\ Hz}$) is negatively correlated with the photochemical quantum yield ($R^2 = 0.7887$, $\alpha < 0.0001$).

Light-Saturated O_2 Evolution Rate. Light-saturated steady-state O_2 evolution rates were measured from whole

dx.doi.org/10.1021/ja5002967 | J. Am. Chem. Soc. 2014, 136, 4048−4055

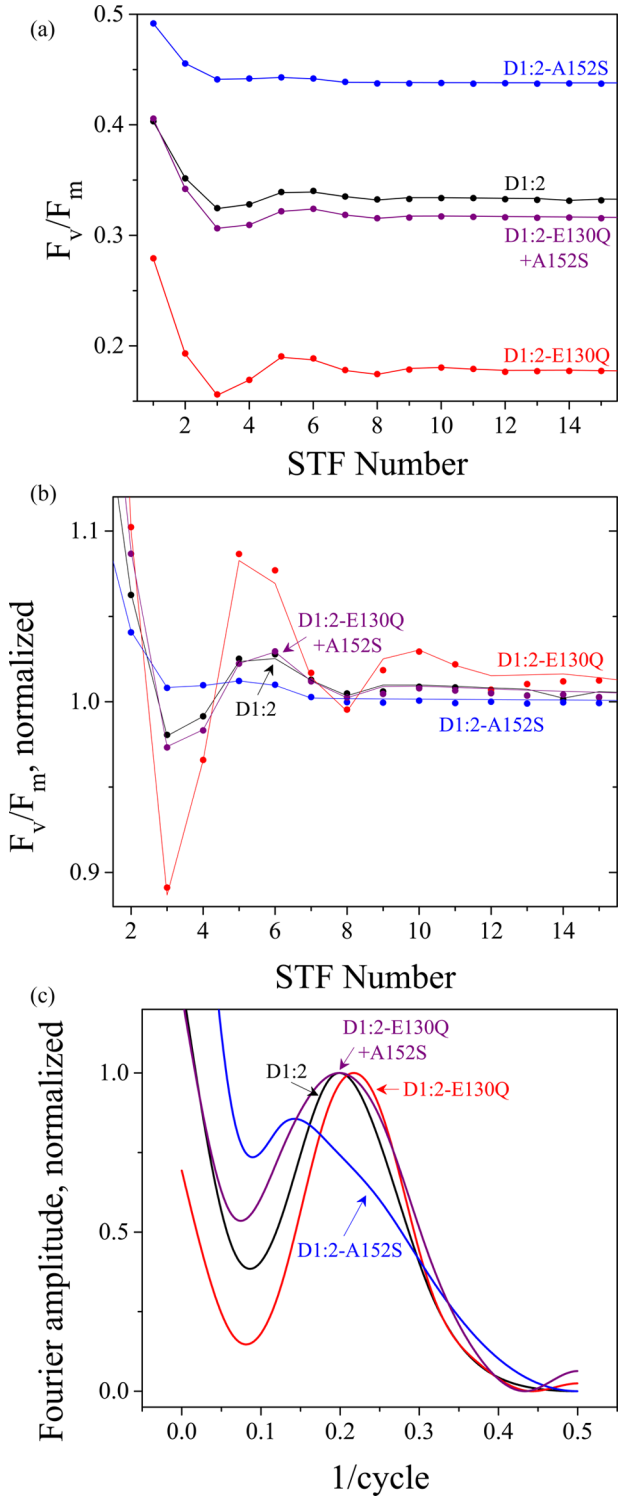

Figure 1. The PSII photochemical quantum yield (F_v/F_m) and WOC turnover efficiency measured at a flash rate of 0.2 Hz ($\gamma_{0.2\ Hz}$) depend on residues Glu/Gln130 and Ala/Ser152. D1:2 (black), D1:2-E130Q (blue), D1:2-A152S (red), and D1:2-A152S+E130Q (violet). (a) F_v/F_m vs single-turnover flash (STF) number. (b) Normalized data illustrating differences in the rates of damping of period-four oscillations and the goodness of fits. Experimental data points are represented as circles and fits (see Methods) as lines. (c) Fourier transforms of F_v/F_m oscillations. Data represent the means of three biological replicates. Full FRR fluorescence traces and fits are shown in Figure S5.

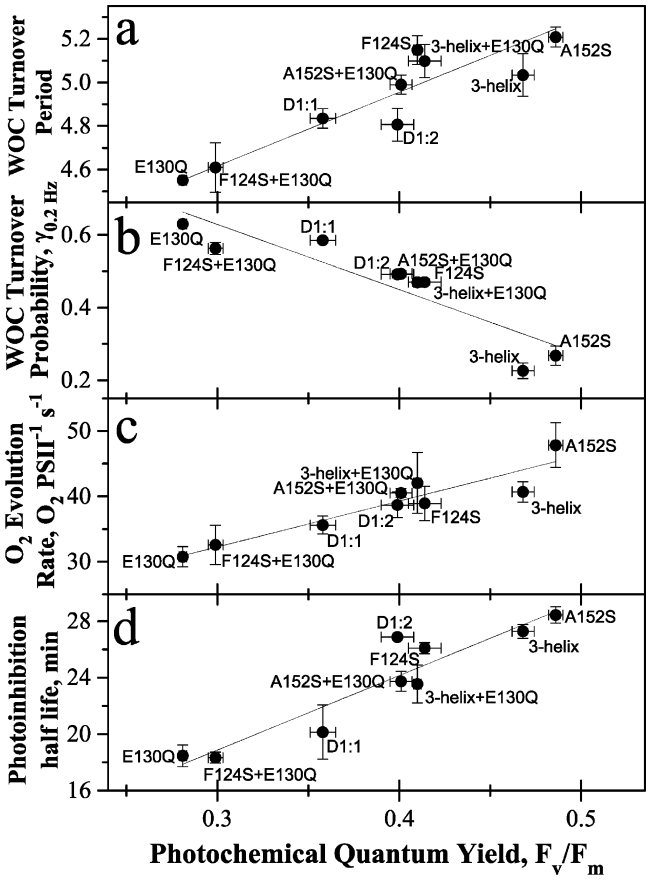

Figure 2. The PSII photochemical quantum yield (F_v/F_m) is inversely proportional to the WOC turnover efficiency measured at a low flash rate where charge recombination contributes, as determined by (a) the model-independent Fourier transform period and (b) the modeled WOC turnover probability ($\gamma_{0.2\ Hz}$); also, F_v/F_m (c) is directly proportional to the light-saturated O_2 evolution rate (in units of O_2 $PSII^{-1}$ s^{-1}) and (d) increases linearly with the half-life of photoinhibition ($t_{1/2}$). Data were fit to linear trend lines with the following equations: (a) $y = 3.39x + 3.60$, $R^2 = 0.9232$; (b) $y = -1.79x + 1.17$, $R^2 = 0.7887$; (c) $y = 52.86x + 3.01$, $R^2 = 0.8594$; and (d) $y = 70.22x + 11.20$, $R^2 = 0.8592$. Full WOC turnover probability data are shown in Figure S5. Full O_2 evolution rate data are shown in Table 1. Full photoinhibition data are shown in Figure S7. Data represent the means of three (WOC turnover efficiency, O_2 evolution rate, photoinhibition half-life) or six (F_v/F_m) biological replicates with standard errors.

cells and normalized to total Chl, and the results are reported in Table 1. Light-saturation curves of O_2 evolution rate versus light intensity for *C.r.*, D1:1, and D1:2 are reported in Figure S6 in the Supporting Information. From knowledge of the Chl/PSII ratios determined by quantitative anti-D1 Western blotting of the thylakoid membranes isolated from these same samples (see Methods), the light-saturated O_2 evolution frequencies (in units of O_2 $PSII^{-1}$ s^{-1}) for these strains were calculated. As shown in Table 1, D1:1 and D1:2 have mean O_2 evolution frequencies of 35.6 and 38.7 O_2 $PSII^{-1}$ s^{-1}, respectively. In D1:2-E130Q, the O_2 evolution rate drops to 30.8 O_2 $PSII^{-1}$ s^{-1}, while in D1:2-A152S it increases to 47.8 O_2 $PSII^{-1}$ s^{-1}. When these two mutations are combined (D1:2-A152S+E130Q), the O_2 evolution rate is 40.5 O_2 $PSII^{-1}$ s^{-1}, which is not significantly different from the D1:2 value when the standard error is taken into account.

Again, the phenotype of D1:2-F124S in terms of O_2 evolution rate was not statistically different from D1:2, nor

dx.doi.org/10.1021/ja5002967 | *J. Am. Chem. Soc.* 2014, 136, 4048−4055

Table 1. Chl/PSII Ratios and WOC Turnover Frequencies Derived from Continuous Light-Saturated O_2 Evolution Measurements[a]

	D1/Chl (fmol/0.1 μg)[b]	Chl/D1[c]	Chl/cell (fmol)	O_2 evolution rate [μmol (mg of Chl)$^{-1}$ h^{-1}][d]	O_2 evolution rate (O_2 PSII^{-1} s^{-1})[e]
C.r.	112 ± 5	1002 ± 45	2.17 ± 0.05	142 ± 11	35.2 ± 1.7
D1:1	96 ± 2	1170 ± 26	1.96 ± 0.07	123 ± 3	35.6 ± 1.4
D1:2	91 ± 7	1230 ± 94	2.02 ± 0.09	126 ± 3	38.7 ± 2.0
D1:2-E130Q	82 ± 6	1369 ± 95	2.34 ± 0.11	90 ± 2	30.8 ± 1.5
D1:2-F124S	77 ± 4	1450 ± 65	2.28 ± 0.08	108 ± 5	38.9 ± 2.6
D1:2-F124S+E130Q	90 ± 8	1249 ± 106	2.60 ± 0.06	104 ± 2	32.6 ± 3.0
D1:2-3-helix	78 ± 4	1438 ± 81	2.36 ± 0.11	114 ± 8	40.7 ± 1.6
D1:2-3-helix+E130Q	71 ± 1	1577 ± 31	2.60 ± 0.04	108 ± 14	42.1 ± 4.7
D1:2-A152S	68 ± 3	1650 ± 81	2.98 ± 0.17	117 ± 13	47.8 ± 3.4
D1:2-A152S+E130Q	69 ± 4	1634 ± 97	2.71 ± 0.07	100 ± 7	40.5 ± 0.7

[a]Data represent means of three biological replicates with standard errors. [b]Quantitative anti-D1 Western blots of thylakoid membrane samples were used to estimate the PSII concentrations (Figure S9). [c]Calculated on the basis of the previous column assuming a molar mass of 893 g/mol for Chl. [d]Light-saturated in vivo rates measured in the presence of 5 mM $NaHCO_3$. [e]Calculated on the basis of the previous columns assuming one D1 per PSII.

was D1:2-F124S+E130Q statistically different from D1:2-E130Q. The 3-helix phenotype (alone or in combination with E130Q) was similar to the A152S phenotype. Figure 2c shows a significant positive correlation between the O_2 evolution rate and the PSII photochemical quantum yield for D1:1, D1:2, and the point mutants (R^2 = 0.8594, α < 0.0001).

Sensitivity to Photoinhibition. Values of the half-life ($t_{1/2}$) for irreversible loss of O_2 evolution (photoinhibition) at high light intensity in the presence of 1 mM lincomycin are presented in Figure 2d (the full traces are shown in Figure S7 in the Supporting Information). In this notation, a longer photoinhibition $t_{1/2}$ represents less sensitivity to photoinhibition (more phototolerance). D1:2 has greater phototolerance than D1:1 ($t_{1/2}$ = 26.9 min vs 20.1 min, respectively), in agreement with previous reports.[9,16,33,35,41−43] D1:2-E130Q is significantly more sensitive to photoinhibition ($t_{1/2}$ = 18.5 min), while D1:2-A152S is less sensitive ($t_{1/2}$ = 28.4 min). D1:2-A152S+E130Q shows an intermediate phenotype with a $t_{1/2}$ of 23.7 min. The F124S mutation does not affect the D1:2 photoinhibition phenotype, and the 3-helix strains closely resemble the A152 strains. Figure 2d shows a significant positive correlation between the photoinhibition $t_{1/2}$ and the PSII photochemical quantum yield for D1:1, D1:2, and the point mutants (R^2 = 0.8592, α < 0.0001).

Growth Phenotypes and D1 Accumulation Levels. All of the point mutants generated in this study were robust and grew photoautotrophically. In order to determine whether the aforementioned phenotypes translate to changes in growth rate or biomass accumulation, growth curves were measured at 80 μE m^{-2} s^{-1}. No significant differences in doubling time among the strains were observed except for D1:2-E130Q and D1:2-F124S+E130Q (Figure 3a; full data are shown in Figure S8 in the Supporting Information). All of the other strains grew with minimal doubling times averaging 6.9 ± 0.1 h, while D1:2-E130Q and D1:2-F124S+E130Q grew 36% and 28% more slowly, respectively. These data show that the reduced growth rate of D1:2-E130Q can be rescued by introducing the 3-helix mutations (D1:2-3-helix+E130Q) or by mutating A152S alone (D1:2-A152S+E130Q).

Natural D1 isoforms (*C.r.*, D1:1, and D1:2) accumulated more biomass at stationary phase than any of the point mutants (Figure 3b and Figure S8 in the Supporting Information). As we previously reported,[16] at low light intensity D1:1 accumulates more biomass at stationary phase (17% more, reported here as dry weight per unit volume) than D1:2 and *C.r.* because of its superior ability to utilize very low photon fluxes (likely through slower kinetics of $P_{680}^+Q_A^-$ charge recombination). In contrast, all seven unnatural point mutations measured herein accumulated substantially less biomass (Figure 3b).

The quantity of PSII in early exponential cells (measured as D1 protein within thylakoid membranes) normalized to total Chl was also higher in the three naturally occurring D1 isoforms (Table 1 and Figure S9 in the Supporting Information). *C.r.* had the lowest Chl/PSII ratio (1002 ± 45) while D1:1 and D1:2 had higher ratios (1170 ± 26 and 1230 ± 94, respectively), in qualitative agreement with our previous study that used much higher cell densities for this measurement.[16] All seven point mutants were higher at 1249 to 1650 Chl/PSII. In addition, *C.r.*, D1:1, and D1:2 had lower total Chl concentrations per cell (2.02−2.17 fmol/cell) compared with the seven point mutants (2.28−2.98 fmol/cell).

DISCUSSION

Our general conclusion from Figure 2 is that among the nine PSII variants studied, those exhibiting a higher yield of PSII charge separation under light-limiting conditions (where charge recombination is significant) have less efficient photochemical turnover, measured both in terms of a lower WOC turnover probability and a longer WOC cycle period. Conversely, these same strains under light saturation (where charge recombination does not compete) confer a correspondingly higher O_2 evolution rate and greater protection against photoinhibition. Taken together, the data clearly establish that PSII primary charge separation is a trade-off between photochemical productivity (water oxidation and plastoquinone reduction) and charge recombination (photoprotection).

We have shown that the presence of both Ser152 and Gln130 in the D1:2 background fully compensate for each other in terms of PSII photochemical quantum yield (F_v/F_m) (Figures 1 and 2), WOC turnover efficiency at low light intensity (and $\gamma_{0.2\ Hz}$) (Figures 1 and 2a,b), O_2 evolution rate (Table 1 and Figure 2c), tolerance to photoinhibition (Figure 2d), and maximal growth rate (Figure 3a). The results obtained from the A152S mutation alone fully account for the phenotypes observed for our original 3-helix mutant in both

dx.doi.org/10.1021/ja5002967 | J. Am. Chem. Soc. 2014, 136, 4048−4055

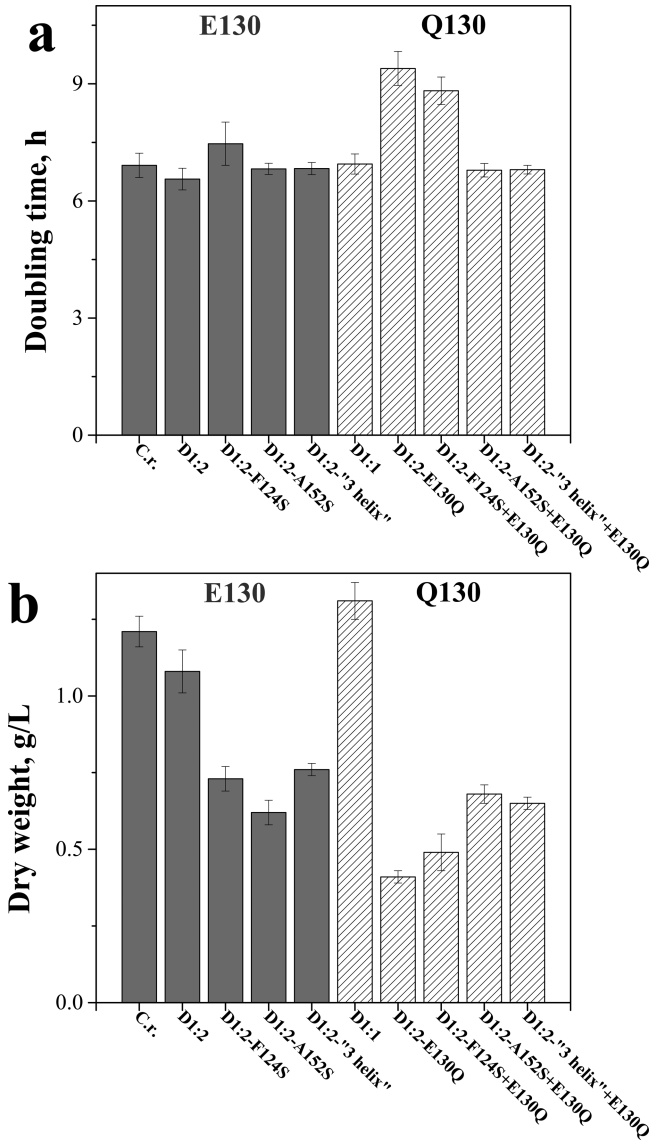

Figure 3. (a) Photoautotrophic doubling times and (b) stationary-phase dry weights of strains containing E130 (gray bars) or Q130 (striped bars) at 80 μE m^{-2} s^{-1} and bubbled with 2% CO_2 in air. Full growth curves are shown in Figure S8. Data represent the means of 4–5 biological replicates with standard errors.

the presence and absence of the E130Q mutation. The D1:2-F124S strain did not vary significantly from D1:2, nor did D1:2-F124S+E130Q vary significantly from D1:2-E130Q.

Correlation plots of the WOC turnover period and WOC turnover probability versus PSII photochemical quantum yield are shown in Figure 2a,b, respectively. Previous studies that have analyzed the charge recombination kinetics and photochemical (charge separation) yield have been limited to no more than three strains.[16−18] Analysis of the seven mutants derived from *Synechococcus* 7942 D1 isoforms and the two natural strains (D1:1 and D1:2) allowed a statistically significant linear correlation to be established over a 3-fold larger range of variants, demonstrating a clear trade-off between these two design variables. We interpret this result using arguments previously hypothesized[22,44,45] and reported:[16,22] a less negative E_m for Pheo/Pheo$^-$ corresponds to a higher quantum yield of photochemistry and faster charge recombination kinetics. Indeed, the values for Pheo/Pheo$^-$ E_m previously measured for D1:1,[22] D1:2,[21] and D1:2-E130Q[20] predict that the magnitude of the energy gap between P_{680}^+/P_{680}* and Pheo/Pheo$^-$ follows the trend D1:2-E130Q < D1:1 < D1:2. The identical trend is observed in the magnitude of F_v/F_m, and the inverse relationship is seen for the WOC turnover period and probability at 0.2 Hz.

The correlation plot of O_2 evolution rate and PSII photochemical quantum yield (Figure 2c) provides statistically significant evidence that the light-saturated rate of PSII water oxidation is linearly correlated with the yield of PSII charge separation. We note that whole-cell O_2 evolution rates do not likely represent the upper kinetic limit of WOC cycling because of limitations in acceptor (PQ) availability and lumenal buffering capacity. However, the in vivo WOC turnover frequencies reported here in the presence of the Calvin–Benson–Bassham cycle acceptor (bi)carbonate follow the same trend (D1:2 > D1:1 > *C.r.*) as previously reported in vitro in the presence of artificial PSII acceptors.[16]

Similarly, the correlation plot of photoinhibition sensitivity and PSII photochemical quantum yield (Figure 2d) shows that a higher yield of PSII photochemistry is directly correlated with increased tolerance to high light fluxes. Sugiura and co-workers recently reported that *T. elongatus* cells expressing D1:2-E130Q are less sensitive to photoinhibition than cells expressing the native D1:2 isoform.[20] In our transgenic *Chlamydomonas* D1 expression system, this experiment produces the opposite result. A redistribution of direct (photoprotective) and indirect ($^1O_2$-generating) charge recombination pathways between the two systems may explain this distinction. Our experimental result (positive correlation of photoinhibition sensitivity with PSII photochemical yield) suggests that the former pathway is dominant, while simulated $S_2Q_A^-$ recombination kinetics in *T. elongatus* suggests that the latter pathway is dominant.[20] This interesting difference deserves more attention in future studies.

The positive correlation between the WOC turnover period at low light and the maximal PSII photochemical quantum yield (Figure 2a) and the negative correlation between the WOC turnover probability at low light and the maximal PSII photochemical quantum yield (Figures 2b) suggest that strains having a more negative Pheo/Pheo$^-$ E_m are better suited for environments where photon flux is limiting. Such conditions are encountered in dense cultures of microalgae and plants or plant parts located below a dense canopy.

On the other hand, the observed positive correlations of both the light-saturated O_2 evolution rate and tolerance to photoinhibition with the maximal PSII photochemical quantum yield (Figure 2c,d) indicate that strains having a less negative Pheo/Pheo$^-$ E_m are best suited for environments of excessive photon flux. Such conditions include dilute cultures of microalgae and sparse plantings of terrestrial crops.

Perhaps the most advantageous strategy for photochemical fitness in light-shifting environments remains the differential expression of *psbA* alleles containing both D1:1 and D1:2. It is interesting to note that no photosynthetic eukaryotes with such a regulatory mechanism have been identified.[46] This may be due to the high rate of homologous recombination and the large number of identical genome copies in chloroplasts, which might hinder the maintenance of highly homologous alleles.[47]

In the 1.9 Å crystal structure of *Thermosynechococcus vulcanus* PSII,[48] D1 position 152 is an Ala located at the D1–CP43 interface (Figure 4). The methyl side chain is 3.4 Å from the phenyl group of CP43-Phe435, which supports the generally hydrophobic interaction between the D1 and CP43 subunits.

dx.doi.org/10.1021/ja5002967 | *J. Am. Chem. Soc.* 2014, 136, 4048–4055

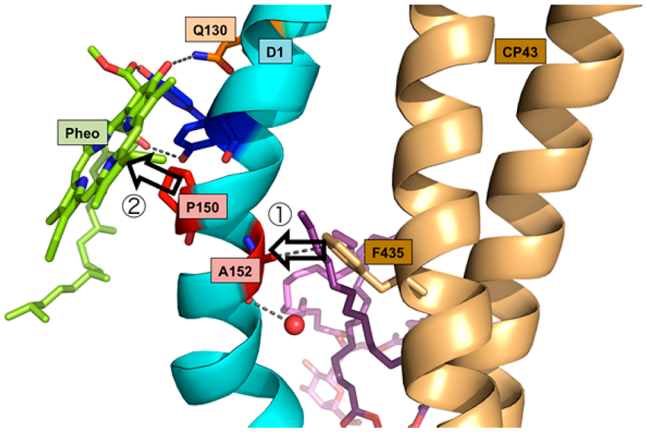

Figure 4. Structural model for the role of D1-152. Arrow 1: When Ser is introduced at position 152, the hydrophobic interaction between D1 and CP43 is less strong, causing the D1 helix to move away from CP43. Arrow 2: Because of the presence of Pro150 trans to position 152, movement of the D1 helix shifts the Pheo binding pocket, thus changing its midpoint potential. The image was generated in PyMOL using coordinates from Umena et al.[48] Purple sticks represent glycolipids; the red sphere is a water bound to the backbone carbonyl oxygen of A152; blue sticks represent D1-Y126 and D1-Y147, which are hydrogen-bonded to Pheo.

As shown, approximately 200° "up" (toward the stroma) from Ala152 there is a conserved proline residue in the α helix (D1-150) that introduces a characteristic bend in the helical structure. This bend provides part of the binding pocket for Pheo. We hypothesize that when Ala152 is mutated to Ser, the CP43−D1 interface becomes less hydrophobic, causing a conformational change in D1, CP43, or both. If the D1 α helix were to move away from CP43, the Pheo binding pocket would be structurally altered as a result of the presence of Pro150 trans to Ser152. It is clear that such an alteration of the protein environment surrounding Pheo would alter its redox properties. Our data suggest that the Pheo/Pheo$^-$ E_m could be less negative in the presence of Ser152. This hypothesis will require additional experimentation for confirmation and is presented here as a working model.

Changes to the midpoint potential of Pheo/Pheo$^-$ may be achieved by altering D1 position 130 (Glu or Gln)[17−20] or possibly position 152 (Ala or Ser). However, we caution that while the intrinsic parameters measured here (PSII photochemical quantum yield, WOC turnover period, WOC turnover probability, O_2 evolution rate, and tolerance to photoinhibition) on early exponential cultures clearly support this argument, these effects are not universally translated to gains in biomass accumulation at the one light intensity tested. Otherwise, all nine analyzed D1:2 sequences coding for the high-light isoform would be expected to contain Ser rather than Ala at position D1-152 because of its favorable influence on high-light performance (Figure 2c,d).

Microalgae are predicted to achieve solar (full incident spectrum) to biomass conversion efficiencies of 5−9% in engineered bioreactors.[49] These efficiencies are comparable to the approximately 6% maximum efficiency calculated for C4 plants.[50] Unfortunately, they are relatively low compared with current photovoltaic technologies[51] and limit the commercial viability of renewable biofuels and reduce total food crop production. In this study, our large sample size of D1 point mutants generated in a single biological background enabled the identification of several design principles that could be applied in the bioengineering of cyanobacteria, algae, and plants for improved photosynthetic efficiencies.

CONCLUSION

We have shown that Ser152 and Gln130 have opposite and complementary effects on the efficiency of PSII, which likely act by altering the E_m of Pheo/Pheo$^-$. These results introduce D1 position 152 as a key determinant of photochemical efficiency and reveal key design principles for maximizing the efficiency of photosynthesis in diverse environments. By studying a large set of D1 point mutants in a single background, we have shown that the WOC turnover efficiency at low light is inversely proportional to the maximal PSII photochemical quantum yield, presumably reflecting a general design limitation of PSII reaction centers. Additionally, the light-saturated O_2 evolution rate and tolerance to photoinhibition are directly proportional to the PSII photochemical quantum yield, thus revealing parallel optimizations of these parameters as a design criterion of natural selection.

ASSOCIATED CONTENT

Supporting Information

FRR fluorometry methods and data analysis summary (Figure S1); mutation construction scheme (Figure S2); localization of point mutations (Figure S3); logo alignments (Figure S4); full FRR fluorescence data and fits (Figure S5); light-saturation curves (Figure S6); full photoinhibition data (Figure S7); growth curves (Figure S8); and anti-D1 Western blots (Figure S9). This material is available free of charge via the Internet at http://pubs.acs.org.

AUTHOR INFORMATION

Corresponding Author

dismukes@rci.rutgers.edu

Present Address

[⊥]D.J.V.: Department of Chemistry, Yale University, New Haven, Connecticut 06520, United States.

Author Contributions

[#]D.J.V. and J.G. contributed equally.

Notes

The authors declare no competing financial interest.

ACKNOWLEDGMENTS

This work was supported in part by the Division of Chemical Sciences, Geosciences, and Biosciences, Office of Basic Energy Sciences, U.S. Department of Energy (Grant DE-FG02-10ER16195 to G.C.D.) and the U.S. Department of Energy [Grant DE-EE0003373, Consortium for Algal Biofuels Commercialization (CAB-COMM), to S.P.M.]. D.J.V. was supported by the Department of Defense, Army Research Office, through a National Defense Science and Engineering Graduate (NDSEG) Fellowship (32CFR168a) and a National Science Foundation Graduate Research Fellowship (DGE-0937373). J.G. was supported by a fellowship from the Comisión Nacional de Investigación Científica y Tecnológica de Chile (CONICYT). We thank Dr. Leslie Vogt for helpful discussions.

REFERENCES

(1) Muh, F.; Zouni, A. *Front. Biosci.* **2011**, *16*, 3072.

(2) Vinyard, D. J.; Ananyev, G. M.; Dismukes, G. C. *Annu. Rev. Biochem.* **2013**, *82*, 577.
(3) Holland, H. D. *Philos. Trans. R. Soc. London, Ser. B* **2006**, *361*, 903.
(4) Falkowski, P. G.; Godfrey, L. V. *Philos. Trans. R. Soc. London, Ser. B* **2008**, *363*, 2705.
(5) Mulo, P.; Sicora, C.; Aro, E.-M. *Cell. Mol. Life Sci.* **2009**, *66*, 3697.
(6) Bustos, S. A.; Schaefer, M. R.; Golden, S. S. *J. Bacteriol.* **1990**, *172*, 1998.
(7) Schaefer, M. R.; Golden, S. S. *J. Bacteriol.* **1989**, *171*, 3973.
(8) Schaefer, M. R.; Golden, S. S. *J. Biol. Chem.* **1989**, *264*, 7412.
(9) Campbell, D.; Eriksson, M.-J.; Oquist, G.; Gustafsson, P.; Clarke, A. K. *Proc. Natl. Acad. Sci. U.S.A.* **1998**, *95*, 364.
(10) Tsinoremas, N. F.; Schaefer, M. R.; Golden, S. S. *J. Biol. Chem.* **1994**, *269*, 16143.
(11) Campbell, D.; Zhou, G.; Gustafsson, P.; Oquist, G.; Clarke, A. K. *EMBO J.* **1995**, *14*, 5457.
(12) Sippola, K.; Aro, E.-M. *Plant Mol. Biol.* **1999**, *41*, 425.
(13) Sicora, C. I.; Ho, F. M.; Salminen, T.; Styring, S.; Aro, E.-M. *Biochim. Biophys. Acta* **2009**, *1787*, 105.
(14) Summerfield, T. C.; Toepel, J.; Sherman, L. A. *Biochemistry* **2008**, *47*, 12939.
(15) Golden, S. S.; Brusslan, J.; Haselkorn, R. *EMBO J.* **1986**, *5*, 2789.
(16) Vinyard, D. J.; Gimpel, J.; Ananyev, G. M.; Cornejo, M. A.; Golden, S. S.; Mayfield, S. P.; Dismukes, G. C. *J. Biol. Chem.* **2013**, *288*, 5451.
(17) Merry, S. A. P.; Nixon, P. J.; Barter, L. M. C.; Schilstra, M.; Porter, G.; Barber, J.; Durrant, J. R.; Klug, D. R. *Biochemistry* **1998**, *37*, 17439.
(18) Rappaport, F.; Guergova-Kuras, M.; Nixon, P. J.; Diner, B. A.; Lavergne, J. *Biochemistry* **2002**, *41*, 8518.
(19) Cser, K.; Vass, I. *Biochim. Biophys. Acta* **2007**, *1767*, 233.
(20) Sugiura, M.; Azami, C.; Koyama, K.; Rutherford, A. W.; Rappaport, F.; Boussac, A. *Biochim. Biophys. Acta* **2014**, *1837*, 139.
(21) Kato, Y.; Sugiura, M.; Oda, A.; Watanabe, T. *Proc. Natl. Acad. Sci. U.S.A.* **2009**, *106*, 17365.
(22) Sugiura, M.; Kato, Y.; Takahashi, R.; Suzuki, H.; Watanabe, T.; Noguchi, T.; Rappaport, F.; Boussac, A. *Biochim. Biophys. Acta* **2010**, *1797*, 1491.
(23) Gimpel, J.; Mayfield, S. *Appl. Microbiol. Biotechnol.* **2013**, *97*, 4499.
(24) Manuell, A. L.; Beligni, M. V.; Elder, J. H.; Siefker, D. T.; Tran, M.; Weber, A.; McDonald, T. L.; Mayfield, S. P. *Plant Biotechnol. J.* **2007**, *5*, 402.
(25) Ho, S. N.; Hunt, H. D.; Horton, R. M.; Pullen, J. K.; Pease, L. R. *Gene* **1989**, *77*, 51.
(26) Nour-Eldin, H. H.; Geu-Flores, F.; Halkier, B. A. In *Plant Secondary Metabolism Engineering*; Fett-Neto, A. G., Ed.; Springer: New York, 2010; p 185.
(27) Sueoka, N. *Proc. Natl. Acad. Sci. U.S.A.* **1960**, *46*, 83.
(28) Zwietering, M. H.; Jongenburger, I.; Rombouts, F. M.; Van't Riet, K. *Appl. Environ. Microbiol.* **1990**, *56*, 1875.
(29) Porra, R. J.; Thompson, W. A.; Kriedemann, P. E. *Biochim. Biophys. Acta* **1989**, *975*, 384.
(30) Mayfield, S. P.; Cohen, A.; Danon, A.; Yohn, C. B. *J. Cell Biol.* **1994**, *127*, 1537.
(31) Ananyev, G.; Dismukes, G. C. *Photosynth. Res.* **2005**, *84*, 355.
(32) Vinyard, D. J.; Zachary, C. E.; Ananyev, G.; Dismukes, G. C. *Biochim. Biophys. Acta* **2013**, *1827*, 861.
(33) Ogami, S.; Boussac, A.; Sugiura, M. *Biochim. Biophys. Acta* **2012**, *1817*, 1322.
(34) Singh, M.; Satoh, K. *Indian J. Biochem. Biophys.* **2003**, *40*, 108.
(35) Tichy, M.; Lupinkov, L.; Sicora, C.; Vass, I.; Kuvikova, S.; Prasil, O.; Komenda, J. *Biochim. Biophys. Acta* **2003**, *1605*, 55.
(36) Kós, P. B.; Deák, Z.; Cheregi, O.; Vass, I. *Biochim. Biophys. Acta* **2008**, *1777*, 74.
(37) Sicora, C. I.; Appleton, S. E.; Brown, C. M.; Chung, J.; Chandler, J.; Cockshutt, A. M.; Vass, I.; Campbell, D. A. *Biochim. Biophys. Acta* **2006**, *1757*, 47.
(38) Nakao, M.; Okamoto, S.; Kohara, M.; Fujishiro, T.; Fujisawa, T.; Sato, S.; Tabata, S.; Kaneko, T.; Nakamura, Y. *Nucleic Acids Res.* **2010**, *38*, D379.
(39) Falkowski, P. G.; Raven, J. A. *Aquatic Photosynthesis*, 2nd ed.; Princeton University Press: Princeton, NJ, 2007.
(40) Montgomery, D. C.; Runger, G. C. *Applied Statistics and Probability for Engineers*; John Wiley & Sons: New York, 1999.
(41) Clarke, A. K.; Soitamo, A.; Gustafsson, P.; Oquist, G. *Proc. Natl. Acad. Sci. U.S.A.* **1993**, *90*, 9973.
(42) Kulkarni, R. D.; Golden, S. S. *J. Bacteriol.* **1994**, *176*, 959.
(43) Sander, J.; Nowaczyk, M.; Buchta, J.; Dau, H.; Vass, I.; Deak, Z.; Dorogi, M.; Iwai, M.; Rogner, M. *J. Biol. Chem.* **2010**, *285*, 29851.
(44) Rutherford, A. W.; Osyczka, A.; Rappaport, F. *FEBS Lett.* **2012**, *586*, 603.
(45) Vass, I.; Cser, K. *Trends Plant Sci.* **2009**, *14*, 200.
(46) Mulo, P.; Sakurai, I.; Aro, E. *Biochim. Biophys. Acta* **2012**, *1817*, 247.
(47) Maréchal, A.; Brisson, N. *New Phytol.* **2010**, *186*, 299.
(48) Umena, Y.; Kawakami, K.; Shen, J.-R.; Kamiya, N. *Nature* **2011**, *473*, 55.
(49) Janssen, M.; Tramper, J.; Mur, L. R.; Wijffels, R. H. *Biotechnol. Bioeng.* **2003**, *81*, 193.
(50) Zhu, X.-G.; Long, S. P.; Ort, D. R. *Annu. Rev. Plant Biol.* **2010**, *61*, 235.
(51) Blankenship, R. E.; Tiede, D. M.; Barber, J.; Brudvig, G. W.; Fleming, G.; Ghirardi, M.; Gunner, M. R.; Junge, W.; Kramer, D. M.; Melis, A.; Moore, T. A.; Moser, C. C.; Nocera, D. G.; Nozik, A. J.; Ort, D. R.; Parson, W. W.; Prince, R. C.; Sayre, R. T. *Science* **2011**, *332*, 805.